



Trade Science Inc.

ISSN : 0974 - 7486

Volume 9 Issue 1

# Materials Science

An Indian Journal

Full Paper

MSAIJ, 9(1), 2013 [1-7]

## Machinability of A356/Al<sub>2</sub>O<sub>3</sub> cast aluminum metal matrix nanocomposites (MMCs)

E.Y.El-Kady, T.S.Mahmoud\*, M.H.G.Ghaith

Department of Mechanical Engineering, King Khalid University (KKU), Abha, Kingdom of Saudi Arabia (KSA)

Received: 15<sup>th</sup> April, 2012 ; Accepted: 4<sup>th</sup> October, 2012

### ABSTRACT

The aim of the present investigation is to study the machinability of A356/Al<sub>2</sub>O<sub>3</sub> nanocomposites under dry machining conditions. The A356/Al<sub>2</sub>O<sub>3</sub> nanocomposites specimens were originally fabricated using a combination between the rheocasting and squeeze casting routes. The nanocomposites were reinforced with Al<sub>2</sub>O<sub>3</sub> particulates having 60 and 200 nm having different volume fractions up to 5 vol.-%. The machinability of the A356/Al<sub>2</sub>O<sub>3</sub> nanocomposites was investigated through measuring the cutting force components ( $F_a$ ,  $F_r$  and  $F_c$ ), tool flank wear, surface roughness of the machined specimens and the chip deformation ratio. The machinability parameters were obtained under different machining conditions. The inserts manufactured from coated carbides were used for machining the nanocomposites. The results revealed that the machinability of nanocomposites was improved by increasing the volume fraction and/or decreasing the nanoparticulates size. However, the cutting force components as well as the flank tool wear increase with increasing the volume fraction and/or the nanoparticulates size.

© 2013 Trade Science Inc. - INDIA

### KEYWORDS

Metal matrix  
nanocomposites;  
Machinability;  
Aluminum alloys;  
Flank tool wear;  
Chip deformation ratio;  
Surface roughness.

### INTRODUCTION

Conventional metal matrix composites (MMCs) have attracted great attention in automotive and aerospace industries due to their high tensile and fatigue strengths, modulus of elasticity, higher micro-plastic strain resistance, adjustable heat conductivity and thermal expansibility<sup>[1,2]</sup>. As composites contain very high hardness strengthening particles, the cutting tool tends to wear severely resulting in difficulties in machining<sup>[3]</sup>. Thus, in manufacturing, difficulties associated with precision and highly efficient machining of composite materials have become an important issue. Turning and

milling operations are among the most common machining operations performed in automotive, aerospace and other application industries. Nowadays, interest is growing in producing composites reinforced by nanoparticulates either by adding these particulates to liquid metals or by in situ techniques. Many researches<sup>[4-7]</sup> have claimed enhanced properties for the produced composites relative to those produced by reinforcing with the micro-particles.

Casting, as a liquid phase process, is capable of producing products with complex shapes<sup>[6]</sup>. It will be attractive to produce as-cast lightweight bulk components of nanocomposites with uniform reinforcement

## Full Paper

distribution and structural integrity. However, nano-sized ceramic particles present difficult problems. It is extremely difficult to obtain uniform dispersion of nano-sized ceramic particles in liquid metals due to high viscosity, poor wettability in the metal matrix, and a large surface-to-volume ratio. These problems induce agglomeration and clustering. The rheocasting (compcasting), as a semi-solid phase process, can produce much better quality nanocomposites compared with conventional casting technique<sup>[5-7]</sup>. In the present investigation the rheocasting technique was used to fabricate A356/Al<sub>2</sub>O<sub>3</sub> nanocomposites. To reduce the porosity of the previously fabricated nanocomposites, a squeezing process was performed. It has been found that such secondary process assisted in reducing significantly the porosity content of the nanocomposites<sup>[5,6]</sup>.

While considerable work has been done on the machinability of conventional composites reinforced with microsize ceramic particulates<sup>[3,8-10]</sup>, very little studies have been conducted to study the machinability of nanocomposites. Generally, it has been found that the selection of cutting tools and cutting conditions represents an essential element in process planning for machining.

In the present investigation, the dry machining characteristics of the A356/Al<sub>2</sub>O<sub>3</sub> nanocomposites were studied during turning. The machining parameters such as the cutting force components, the flank tool wear, the surface roughness of the machined specimens, and the chip deformation ratio were extensively studied.

### EXPERIMENTAL PROCEDURES

The A356 Al-Si-Mg cast alloy was used as a matrix. The chemical composition of the A356 Al alloy is listed in TABLE 1. Nano-Al<sub>2</sub>O<sub>3</sub> particulates were used as reinforcing agents. The Al<sub>2</sub>O<sub>3</sub> nanoparticulates have two different average sizes, typically, 200 and 60 nm. Several metal matrix nanocomposites (MMNCs) were fabricated with different volume fractions of Al<sub>2</sub>O<sub>3</sub> nanoparticulates

TABLE 1 : The chemical composition of A356 alloy

Alloy	Chemical composition (wt.-%)						
	Si	Fe	Cu	Mn	Mg	Zn	Al
A356	6.6	0.25	0.11	0.002	0.14	0.026	Bal.

up to 5 vol.-%.

The A356/Al<sub>2</sub>O<sub>3</sub> nanocomposites were prepared using a combination of rheocasting and squeeze casting techniques. Preparation of the composite alloy was carried out according to the following procedures: About 1 kg of the A356 Al alloy was melted at 680±2 °C in a graphite crucible in an electrical resistance furnace. After complete melting and degassing by argon gas of the alloy, the alloy was allowed to cool to the semisolid temperature of 602 °C. At such temperature the liquid/solid fraction was about 0.7. The liquid/solid ratio was determined using primarily differential scanning calorimeter (DSC) experiments performed on the A356 alloy. A simple mechanical stirrer with three blades made from stainless steel coated with bentonite clay was introduced into the melt and stirring was started at approximately 1000 rpm. Before stirring the nanoparticulates reinforcements after heating to 400 °C for two hours were added inside the vortex formed due to stirring. After that, preheated Al<sub>2</sub>O<sub>3</sub> nanoparticulates were introduced into the matrix during the agitation. After completing the addition of Al<sub>2</sub>O<sub>3</sub> nanoparticulates, the agitation was stopped and the mixture was poured into preheated tool steel mould and immediately squeezed during solidification. The produced ingot has 30 mm diameter and 130±10 mm length. The nanocomposites were heat treated at T6 before conducting the machining tests. The tested ingots ends were cut using reciprocating saw to adjust the ingots length on 120 mm.

The machinability tests were conducted on a conventional center lathe machine. The lathe has a power of 6.6 kW. The machining processes were conducted through dry cutting using coated sintered carbide inserts of type TK15 (*WidiaKnupp, Poland*). The cutting tool inserts have a geometry of rake angle -5°, clearance angle 5°, setting angle 60°, auxiliary setting angle 60° and nose radius of 0.4 mm were used to conduct the experiments. The machinability parameters such as the cutting force components (axial component,  $F_a$ , radial component,  $F_r$ , and main cutting component,  $F_c$ ), flank tool wear, chip deformation ratio and the surface roughness of the machined surfaces were investigated through different machining conditions. The tests were conducted at several cutting speeds of 45.25, 64.7, 89.85, 125.76, 177.79 and 248.18 m/min. Both the

feed rate and depth of cut were kept constant at 0.11 mm/rev and 1 mm, respectively. The flank tool wear was recorded after machining time of 2.4 min at cutting speed of 196 m/min, depth of cut of 1 mm and feed rate of 0.11 mm/rev. The tool flank wear was measured using tool room microscope.

A three-component dynamometer, (*model 9257BA*) made by *Kistler, Switzerland* was used for measuring the cutting force components  $F_a$ ,  $F_r$  and  $F_c$ . Figure 1 shows a photograph of the dynamometer during calibration. The dynamometer was attached to a control unit that can measure forces up to 10 kN. The cutting force components were recorded directly during machining using *DynoWare* software provided by the dynamometer manufacturer as shown in Figure 2. A stylus type surface roughness measuring instrument (*model SJ-201P*) made by *Mitutoyo, Japan* was used

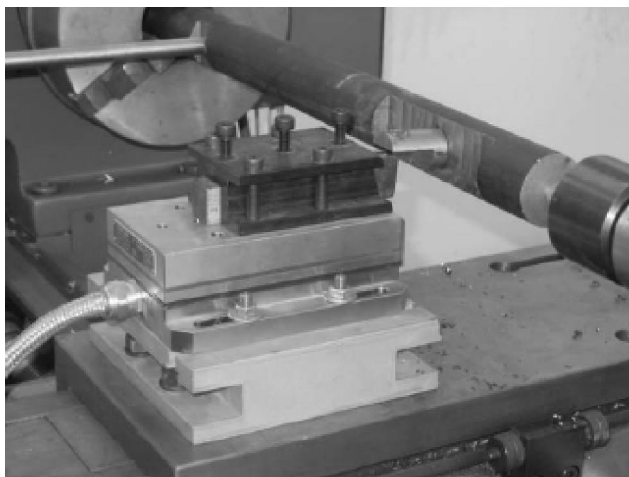


Figure 1 : A photograph of the dynamometer during calibration

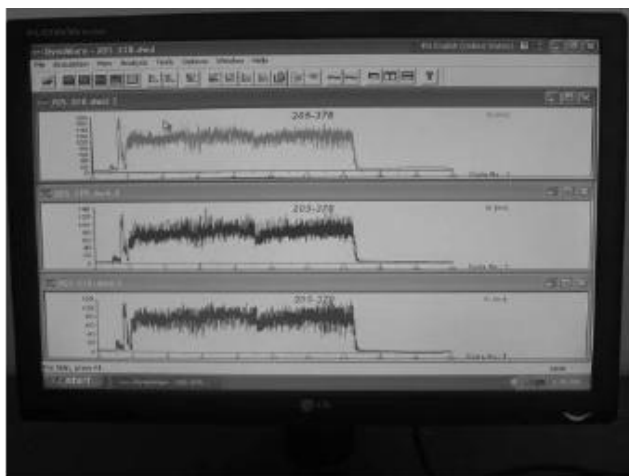


Figure 2 : The cutting force measurement

to measure the surface roughness of the nanocomposites specimens after machining. The surface roughness parameter ( $R_a$ ) was measured. An average of ten readings was considered.

## RESULTS AND DISCUSSION

### Cutting force components measurements

The variation of the cutting force components  $F_a$ ,  $F_r$  and  $F_c$  with the cutting speed is shown in Figure 3. The results showed that, for the unreinforced A356 matrix, the cutting force components have the same values at low cutting speeds (i.e. 45.25 and 64.27 m/min) while a remarkable increase was noticed when the cutting speed changed from 64.27 to 89.85 m/min. After that the cutting force components slightly dropped when the cutting speeds increases from 89.85 to 125.76 m/min. A steady state trend was noticed in the range of cutting speeds of 125.76 to 248.18 m/min. These results were attributed to the formation of built-up edge (B.U.E.) and growth in the range of cutting speeds of 64.27 to 89.85 m/min and it is disappear after 125.76 m/min. The nanocomposites exhibited the same aforementioned behavior of the unreinforced A356 matrix. However, it has been noticed that a slight increase in the values of the cutting force components was recorded for the nanocomposites containing 1 vol.-%, 3 vol.-% and 5 vol.-% of 60 nm  $Al_2O_3$  nanoparticulates relative to that recorded for the unreinforced A356 matrix. Such behavior may attribute to the effect of the reinforcements where the strength of the nanocomposites increases with the increasing of the reinforcement volume fractions<sup>[5]</sup>.

The cutting force components increase by increasing the nanoparticulates size. The results indicated that the B.U.E disappeared during machining the nanocomposites reinforced with 200 nm particulates. These results may due to the increase of the nanocomposites hardness with the increase of the nanoparticulates size. The results revealed that the measured cutting force components when cutting nanocomposites specimens of 200 nm particles size more than that were measured for nanocomposites of 60 nm. Such behavior can be attributed to the effect of particles size on the nanocomposites hardness where

## Full Paper

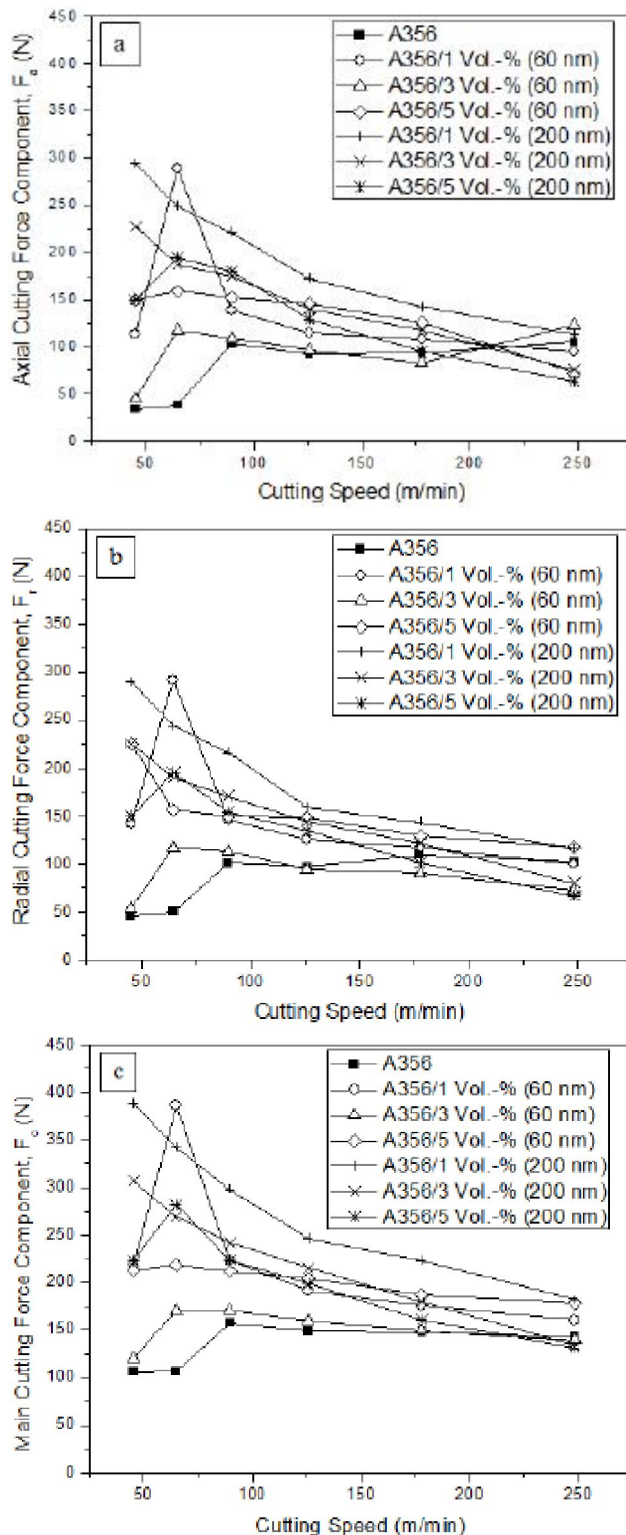


**Figure 3 : Variation of the cutting force components with the cutting speed. (a) axial cutting force component,  $F_a$ , (b) radial cutting force component,  $F_r$ , (c) main cutting force component,  $F_c$**

the hardness of the composites having large particulates sizes more than that of the composites having small

particulates size for the same value of the volume fraction<sup>[5,6]</sup>. The increase of hardness increases the nanocomposites resistance for insert penetration and increases cutting force components

### Chip compression ratio

The obtained chip compression ratio ( $\lambda_c = h_2/h_1$ ) versus the cutting speed for different volume fractions and reinforcement size were graphically represented in Figure 4. The results indicated that the chip compression ratio decreases with the increasing of the cutting speed due to the effect of cutting speed on the strain rate, where the increase of the cutting speeds reduces the machining time, then decreasing the chip compression ratio. The results indicated also that the chip compression ratio of the nanocomposites is more than that of the unreinforced matrix. These results were attributed to the nanocomposites ductility is more than that of the unreinforced matrix as obtained in the previous work by the authors<sup>[5,6]</sup>.

The measured chip compression ratio for the A356/Al<sub>2</sub>O<sub>3</sub> nanocomposites was strongly affected by the volume fraction and the Al<sub>2</sub>O<sub>3</sub> nanoparticulates size as shown in Figure 4. It has been noticed that the nanocomposites specimens containing 1 vol.-% of 60 nm Al<sub>2</sub>O<sub>3</sub> nanoparticulates have higher chip compression ratio than the nanocomposites containing 1 vol.-% of 200 nm Al<sub>2</sub>O<sub>3</sub> nanoparticulates. These results are due to the decrease of the nanoparticulates size increases the nanocomposites ductility of the nanocomposites as reported in Ref.<sup>[6]</sup>. The results showed that the highest chip compression ratio was obtained for nanocomposites containing 1 vol.-% Al<sub>2</sub>O<sub>3</sub> nanoparticulates of 60 nm size. The increasing of the volume fraction to 3 vol.-% and 5 vol.-% reduces the chip compression ratio relative to that obtained for nanocomposites containing 1 vol.-%. These results are related to the increase of the volume fraction to 3 vol.-% and 5 vol.-% increases the nanocomposites strength and hardness then reduces the nanocomposites ductility, so reduces the chip compression ratio. The obtained results recorded also that the particulates size has a remarkable effect on the chip deformation ratio, as noticed from comparing the results obtained in Figure 4 for the nanocomposites specimens of 60 nm and 200 nm particulates size. At the same volume fraction, the

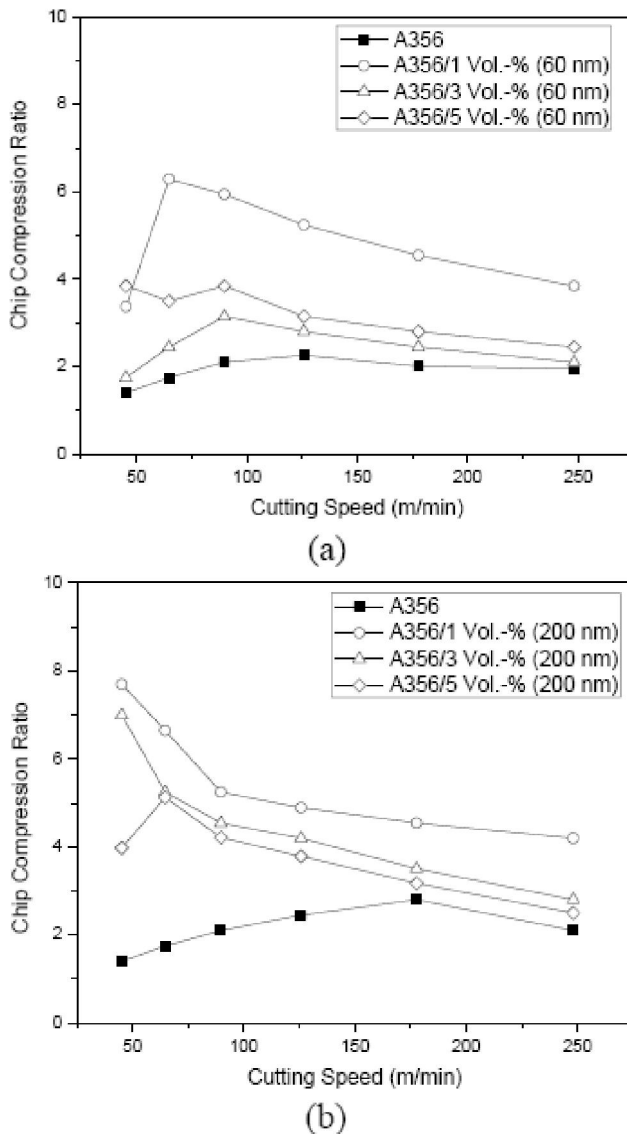


**Figure 4 : Chip compression ratio versus the cutting speed for different volume fractions and reinforcement size of (a) 60 nm and (b) 200 nm**

nanocomposites containing  $\text{Al}_2\text{O}_3$  nanoparticles of 200 nm exhibited higher chip compression ratio compared with the nanocomposites containing  $\text{Al}_2\text{O}_3$  nanoparticles of 60 nm. The increase of the particulates size increases the cutting force components and accordingly the chip deformation ratio was increased. Figure 5 shows sample optical micrographs of the chips formed during machining of the unreinforced as well as the nanocomposites containing different sizes and volume fractions of  $\text{Al}_2\text{O}_3$  nanoparticles.

### Surface roughness

The variation of the surface roughness parameter ( $R_z$ ) with the cutting speed is shown in Figure 6. The

results show that the surface roughness parameter  $R_z$  of the machined specimens was improved by increasing the cutting speed and it deteriorates by increasing the size and volume fraction of the nanoparticles. The increase of the cutting speed reduces the friction forces and the tools wear, so improves the surface roughness. The noticed improvement in the surface roughness with increasing volume fraction may attribute to the increase of the nanocomposites hardness, which improves machinability and roughness. It has been found that the surface roughness parameter  $R_z$  increases with increasing the  $\text{Al}_2\text{O}_3$  nanoparticles size, where the values obtained for the nanocomposites reinforced with 200 nm were higher than those obtained for the nanocomposites reinforced with 60 nm under all the investigated cutting speeds. These results related to the increase of cutting force components with the increasing of the particulates size. The decrease of nanoparticles size reduces the induced vibration and accordingly improves the surface roughness.

### Tool flank wear

Figure 7 shows the flank tool wear versus the volume fractions of the nanocomposites specimens reinforced with different nanoparticles sizes. The obtained results showed that a reasonable performance for the coated carbide inserts in machining the matrix and nanocomposites specimens. However a high flank wear was noticed during cutting of the nanocomposites specimens reinforced with either high volume fractions or reinforcement particulate size. These results were attributed to the increase of the volume fraction of reinforcement increases the hard phase (abrasive media) then increases the number of abrasive particulates scratching the tool, so increases the tool wear<sup>[11,12]</sup>. A higher tool wear was recorded in case of nanocomposites specimen reinforced with 200 nm than that reinforced with 60 nm for all values of volume fractions used in this work. These results are due to the cutting forces required in the case of cutting nanocomposites of 200 nm more than that in the case of nanocomposites of 60 nm, so the heat generated in case of the cutting nanocomposites of 200 nm is higher than that in case of cutting nanocomposites of 60 nm. Hence, in case of cutting nanocomposites specimens of

## Full Paper

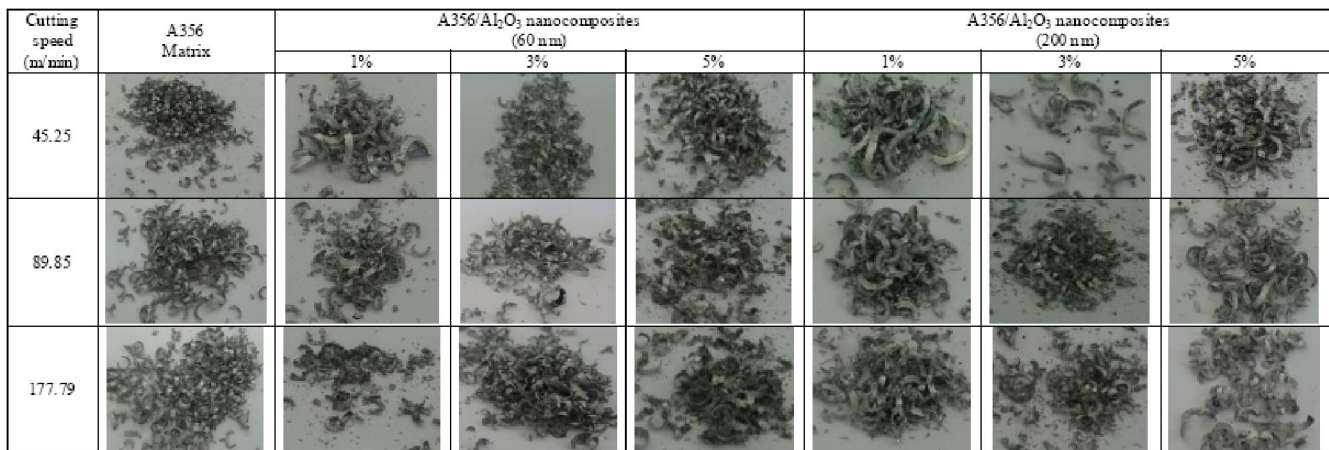
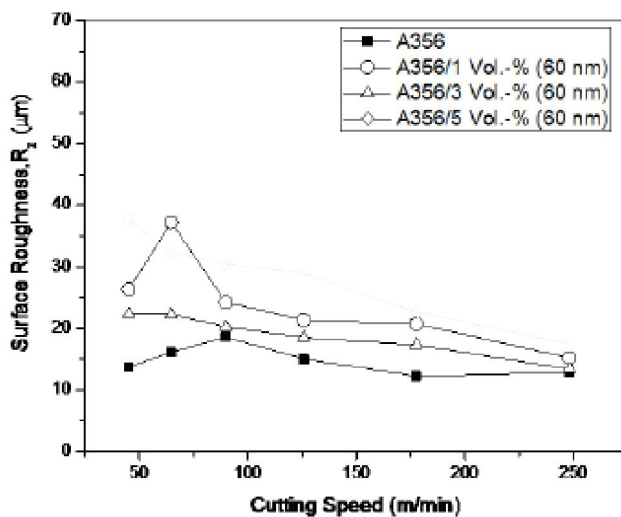
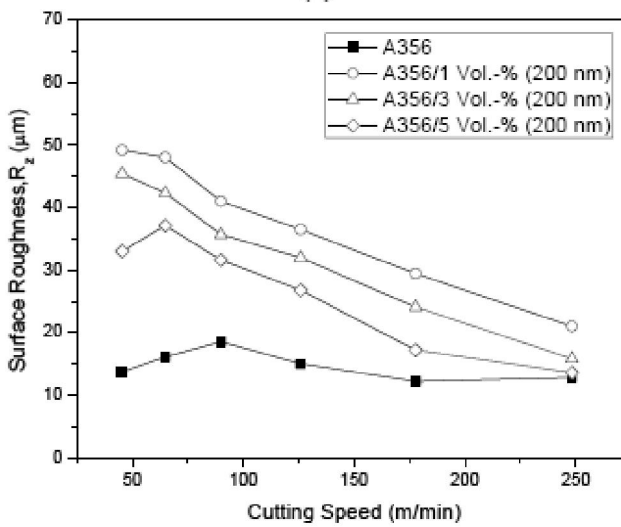


Figure 5 : Optical micrographs of the chips formed during machining of the nanocomposites and A356 unreinforced alloy at several cutting speeds



(a)



(b)

Figure 6 : The variation of the surface roughness parameter ( $R_z$ ) with the cutting speed for different volume fractions and reinforcement size of (a) 60 nm and (b) 200 nm

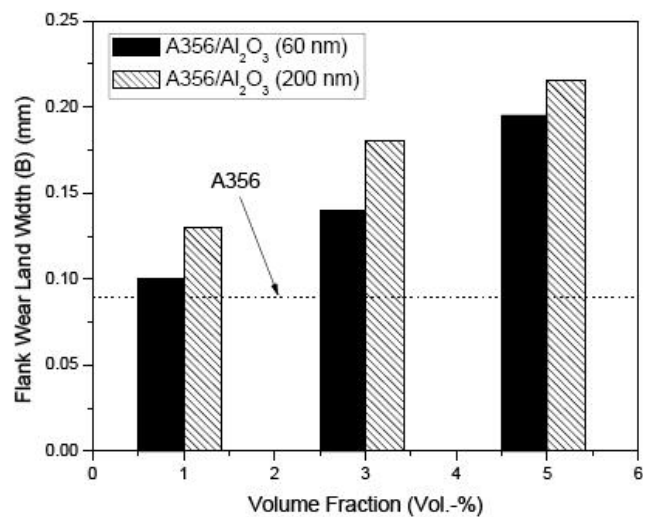


Figure 7 : Variation of the tool flank wear land width with the volume fraction at different nanoparticles sizes

200 nm the recrystallization of built up edge was reached corresponding to a cutting speed smaller than that of the other nanocomposites specimens (of 60 nm).

## CONCLUSIONS

According to the results obtained from the current investigation, the following conclusions can be pointed out:

1. The machinability of A356/Al<sub>2</sub>O<sub>3</sub> nanocomposites was improved by increasing the volume fraction and/or decreasing the Al<sub>2</sub>O<sub>3</sub> nanoparticles size. However, the cutting force components were increased by increasing both the volume fraction and the size of Al<sub>2</sub>O<sub>3</sub> nanoparticles.
2. The surface roughness parameter ( $R_z$ ) of the A356/

Al<sub>2</sub>O<sub>3</sub> nanocomposites was improved by increasing the cutting speed and it deteriorates by increasing the volume fraction and/or the Al<sub>2</sub>O<sub>3</sub> nanoparticulates size.

3. The chip compression ratio of the machined A356/Al<sub>2</sub>O<sub>3</sub> nanocomposites decreases by increasing the volume fraction and/or the Al<sub>2</sub>O<sub>3</sub> nanoparticulates size.
4. The A356/Al<sub>2</sub>O<sub>3</sub> nanocomposites exhibited higher tool flank wear when compared with the A356 unreinforced matrix. The flank tools wear increases by increasing the volume fraction and/or the Al<sub>2</sub>O<sub>3</sub> nanoparticulates size.

### ACKNOWLEDGMENT

This work is supported by the King Abdel-Aziz City of Science and Technology (KACST) through the Science and Technology Center at King Khalid University (KKU), Fund (NAN 08-172-07). The authors thank both KACST and KKU for their financial support. Special Thanks to Prof. Dr. Ahmed Taher, Vice President of KKU, Prof. Dr. Eid Al-Atibi, Dean of the Scientific Research at KKU, and Dr. Khaled Al-Zailaie, Dean of the faculty of engineering at KKU, for their support.

### REFERENCES

- [1] T.W.Clyne; Comprehensive composite materials, In: A.Kelly, C.Zweben, (Eds); Metal Matrix Composites, **3**, Pergamon, Oxford (2000).
- [2] A.S.M.Handbook, Composites, **21**, (2001).
- [3] J.P.Davim; Diamond tool performance in machining metal-matrix composites, Journal of Material Processing Technology, **128**, 100–105 (2002).
- [4] El-Sayed Youssef El-Kady, Tamer Samir Mahmoud, Ali Abdel-Aziz Ali; On the electrical and thermal conductivities of cast A356/Al<sub>2</sub>O<sub>3</sub> metal matrix nanocomposites, Materials Sciences and Applications, **2**, 1180-1187 (2011).
- [5] El-Sayed Youssef El-Kady, Tamer Samir Mahmoud, Mohamed Abdel-Aziz Sayed; Elevated temperatures tensile characteristics of cast A356/Al<sub>2</sub>O<sub>3</sub> nanocomposites fabricated using a combination of rheocasting and squeeze casting techniques, Materials Sciences and Applications, **2**, 390-398 (2011).
- [6] I.S.El-Mahallawi, K.Eigenfield, F.Kouta, A.Hussein, T.S.Mahmoud, R.M.Ragaie, A.Y.Shash, W.Abou-Al-Hassan; Synthesis and characterization of new cast A356/(Al<sub>2</sub>O<sub>3</sub>)P metal matrix nano-composites, ASME, In the proceeding of the 2nd Multifunctional Nanocomposites & Nanomaterials: Int. Conference & Exhibition, organized by the American University in Cairo - AUC, in collaboration with Cairo University, Sharm El Sheikh, Egypt, January 11-13, (2008).
- [7] Yong Yang, Jie Lan, Xiaochun Li; Study on bulk aluminum matrix nano-composite fabricated by ultrasonic dispersion of nano-sized SiC particles in molten aluminum alloy, Mater.Sci.Eng., **380A**, 378–383 (2004).
- [8] Y.Zhu, H.A.Kishawy; Influence of alumina particles on the mechanics of machining metal matrix composites, Int.J.Mach.Tools Manuf, **45**, 389–398 (2005).
- [9] L.Cronjager, D.Meister; Machining of fibre and particle reinforced aluminium, Ann.CIRP, **41(1)**, 63–66 (1992).
- [10] P.Narahari, B.C.Pai, R.M.Pillai; Some aspects of machining cast Al-SiCp composites with conventional high speed steel and tungsten carbide tools, J.Mater.Eng.Perform, **8(5)**, 538–542 (1999).
- [11] E.Y.El-Kady; Machinability of squeeze casting MMCs A390 reinforced with SiC and Al<sub>2</sub>O<sub>3</sub> particulates, Scientific Bulletin, Ain Shams University, Faculty of Engineering, **38(4)**, 867-886 December (2003).
- [12] A.Manna, B.Bhattacharayya; A study on machinability of Al/SiC MMC, Journal of Materials Processing Technology, **140**, 711–716 (2003).